Reaction Rates in a Theory of Mechanochemical Pathways

Wolfgang Quapp*, Josep Maria Bofill†

June 23, 2016

Abstract

If one applies mechanical stress to a molecule in a defined direction then one generates a new, effective potential energy surface (PES). Changes for minima and saddle points by the stress are described by Newton trajectories on the original PES [Quapp and Bofill, Theor. Chem. Acc. **135**, 113 (2016)]. The barrier of a reaction fully breaks down for the maximal value of the norm of the gradient of the PES along a pulling Newton trajectory. This point is named barrier breakdown point (BBP). Depending on the pulling direction, different reaction pathways can be enforced. If the exit saddle point (SP) of the chosen pulling direction is not the lowest SP of the reactant valley, on the original PES, then the SPs must change their role anywhere: in this case the curve of the $log(rate)$ over the pulling force of a forward reaction can show a deviation from the normal concave curvature. We discuss simple, 2-dimensional examples for this model to understand more deeply the mechanochemistry of molecular systems under a mechanical stress.

Keywords: Reaction rate, Effective potential energy surface, Mechanochemistry, Newton trajectory, Barrier breakdown, Saddle, Intermediate. ■

*Department of Mathematics, University Leipzig, PF 100920, D-04009 Leipzig, Germany quapp@uni-leipzig.de

†Departament de Química Inorgànica i Orgànica, Secció de Química Orgànica, Universitat de Barcelona; *and* Institut de Química Teòrica i Computacional, Universitat de Barcelona, (IQTCUB), Martí i Franquès, 1, 08028 Barcelona Spain jmbofill@ub.edu

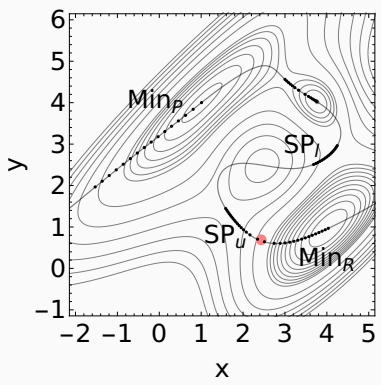

Assume a pulling along the direction of the Newton trajectory from minimum R to minimum P. Shown is an overlay of the stationary points of diverse effective surfaces under the pulling. Used are 16 equidistant loads. The red point is the final barrier breakdown point of the direction. An upper saddle moves downward, but a lower saddle moves uphill: so, the common rate of a forward reaction can become abnormal. Level lines of the original PES are shown as background where around the minimums dense lines are used.

INTRODUCTION

Considerable interest is attached to the problem of a mechanical stress applied to a molecular system. In theoretical chemistry there are two basic concepts underlying many widely used models, namely, the potential energy surface (PES) and the reaction path (RP). The RP is a one-dimensional description of a chemical reaction through a sequence of molecular geometries in an N-dimensional configuration space. We use $N = 3n - 6$ for the number of non-redundant internal coordinates, and n is the number of the atoms of the molecular system. An interesting type of RP models is the Newton trajectory (NT).[1–8] For this type of RP holds that at every point of the curve the gradient of the PES points into the same direction, a direction of a prescribed search vector. On the other hand, this property is the central idea of models of mechanochemical stress applied to a molecular system where the search direction is now the direction of the stress vector. This is the reason why NTs should be taken into account as the basic model of a great variety of mechanochemical problems.[9] The present study is a follow-up of a first investigation of the realm of mechanochemistry with the NTs tool.[10]

In the last years, the phenomena of the action of a mechanical stress over a molecular system have motivated experimental and theoretical research,[11–19] and see further references therein. We will quantify molecular stress geometrically. Basically, the model was created by Ong et al.[20] and it was treated independently by Ribas-Ariño et al.[21] and Wolinski and Baker.[22] Now it is the generally accepted model.[14,18,23,24] It consists in a first order perturbation on the associated PES of the unperturbed molecular system due to a stress or pulling force, $\mathbf{f}$, by

$$V_f(\mathbf{r}) = V(\mathbf{r}) - \mathbf{f}^T (\mathbf{r} - \mathbf{r}_o) \ , \tag{1}$$

where the symbol T means transposition of a vector or a matrix. The scalar product with the force, $\mathbf{f}$, ensures that only the part of $\mathbf{r} - \mathbf{r}_o$ in the direction of $\mathbf{f}$ acts on the system. The subtrahend in Eq.1 is a hyperplane in the space $\mathbb{R}^{N+1}$ which is sloped in the direction of the force, $\mathbf{f} \in \mathbb{R}^N$. V_f is named the force-modified PES,[20] the force-transformed PES,[14,25] or the effective PES. A similar model was discussed by Thornton[26] for the prediction of the effect of substituent changes on the transition state (TS) geometry. It can also be thought

as the change of the PES of a reaction under catalytic conditions. In this case, the direction and the magnitude of vector $\mathbf{f}$ are fixed for every special catalyst. A combination of both aspects is mechanocatalysis.[27]

METHODOLOGY

For a given force, $\mathbf{f}$, we have an effective PES, V_f, which has a new inherent chemistry with respect to the unperturbed PES, V, such as other reaction rates and other chemical properties. Of course, the linear perturbation in Eq.1 is the simplest model.[28] Meanwhile, time was used to derive new basic ideas of mechanochemistry.[14,28–33] The force $\mathbf{f}$ in Eq.1 may be determined by the change of a distance between two pulling points of the molecule,[34] or by any other experimental setup. Formerly it was associated with one of the $N = 3n-6$ internal coordinates[34] or a linear combination of them.[20] Throughout the present work we assume that the plane of two intrinsic coordinates (x, y) is the stage where the pulling works. These coordinates may describe the weakest point of a molecule where it breaks preferentially.[35] We note that the theory and the use of NTs can be applied to N-dimensional systems.[2,36] All formulas in this section hold for the N-dimensional case.

Due to the external force, the stationary points are located at different positions on the effective potential, $V_f(\mathbf{r})$,[32] with respect to the unperturbed potential, $V(\mathbf{r})$, where it holds $\nabla_{\mathbf{r}} V(\mathbf{r}) = \mathbf{g}(\mathbf{r}) = \mathbf{0}$. The stationary points on the effective potential have to satisfy the analogous condition, $\nabla_{\mathbf{r}} V_f(\mathbf{r}) = \mathbf{0}$. Since $V_f(\mathbf{r})$ is the one given in Eq.1 it follows that the new minimums or SPs should satisfy

$$\nabla_{\mathbf{r}} V_f(\mathbf{r}) = \mathbf{0} = \mathbf{g} - \mathbf{f} \ . \tag{2}$$

One searches a point where the gradient of the original PES, $\mathbf{g}$, has to be equal to the mechanochemical force, $\mathbf{f}$, being the force that induces the chemical process. If the mechanical stress in a defined direction is $\mathbf{f} = F\mathbf{l}$ with a fixed unit vector, $\mathbf{l}$, then it is $\mathbf{l} = \mathbf{g}/|\mathbf{g}|$ and $F = |\mathbf{g}|$ is the magnitude at the stationary points since from Eq.2 we have, $\mathbf{0} = \mathbf{l}\,(|\mathbf{g}| - F)$, being satisfied if the former equality is also satisfied. Eq.2 means that the tangential hyperplane to the original PES, characterized by the gradient, $\mathbf{g}$, is equal to the hyperplane of

the pulling force, $\mathbf{f}^T\mathbf{r}$, in Eq.1, see Fig.1, and compare Fig.12a in ref. 14. The case $F = 0$ is named the thermal limit.[14] It is the case without a mechanical load.

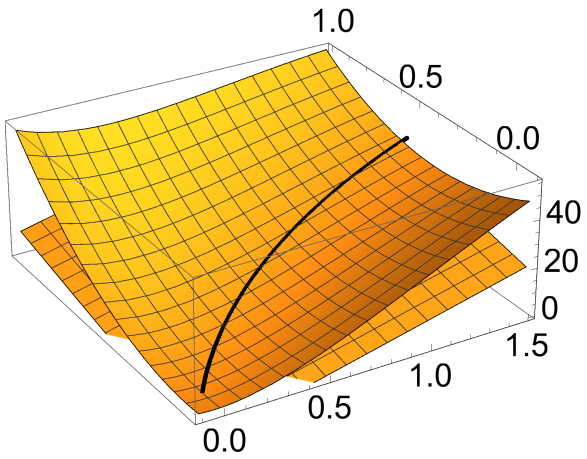

Figure 1: PES with an NT, and a tangential plane to direction $\mathbf{l}$ of the NT. The tangential plane touches the PES at a point of the NT which moves with a changing F along the NT.

We also use the alternate mathematical form for the solution of Eq.2 by the projector equation[1,2,5]

$$\left[\mathbf{U} - \mathbf{l}\mathbf{l}^T\right]\mathbf{g} = \mathbf{0} \tag{3}$$

where $\mathbf{U}$ is the unit matrix. The equation has to hold unattached from the uncomfortable norm, $|\mathbf{g}|$, and it means nothing else that the vectors $\mathbf{g}$ and $\mathbf{l}$ are parallel. It holds $\mathbf{g} = \mathbf{f} = \mathbf{l}F = \mathbf{l}|\mathbf{g}|$. Note that at the stationary points of $V_f(\mathbf{r})$, Eq.3 is fulfilled, because $|\mathbf{g}| - F = 0$, and from this it is $(\mathbf{g} - \mathbf{f}) = \mathbf{0}$.

Now we treat a fixed direction of $\mathbf{l}$, but different magnitudes of the forces, F. For point-to-point changing forces, F, we should get a curve of the 'reaction path following force displaced stationary points (FDSPs)'.[23] The minimums and the SPs of index one of the effective PES are on the FDSPs curve, because at these points holds $|\mathbf{g}| = F$. The FDSPs are a solution of Eq.3, but this equivalently means that they are on the solution of the differential equation of Branin[37] which we can use in $N = 3n - 6$ nonredundant coordinates[9,10]

$$\frac{d\mathbf{r}}{dt} = \pm\mathbf{A}(\mathbf{r})\,\mathbf{g}(\mathbf{r}) \ . \tag{4}$$

t is a curve parameter and the matrix $\mathbf{A}$ is constructed as a product of the determinant of the Hessian, $\mathbf{H}$, with the inverse Hessian,

$$\mathbf{A} = Det(\mathbf{H})\,\mathbf{H}^{-1}\ . \tag{5}$$

The determinant is a scalar. Its zero removes the singularity of $\mathbf{H}^{-1}$ emerging on the way to the SP. The matrix $\mathbf{A}$ is named the desingularized inverse Hessian, or the adjoint to $\mathbf{H}$. The signs '$\pm$' are used to allow the curve to go uphill from a minimum, or downhill from an SP. Curves $\mathbf{r}(t)$ satisfying this expression are called *Newton trajectories* (NT). A property of Eq.4 is that the gradient at every curve point always points into the same direction, $\mathbf{l}$, if it had this direction at an initial point. Then holds the parallelity of the vectors, $\mathbf{l}||\mathbf{g}$, throughout the path.[1,2] It also means that the solution is a distinguished coordinate path,[1,2,38] as well as a solution of the projector Eq.3.

The solution curve of the Branin equation is *a regular curve* from a point near the minimum to an SP if no valley-ridge inflection point is crossed.[2] The Branin Eq.4 is a well-known model for RPs.[1,2,5,8] This RP model is especially used here for the FDSPs: for every special magnitude of the force, F, we get a moved stationary point of the new effective potential, $V_f(\mathbf{r})$ with $\mathbf{f} = F\mathbf{l}$ and $\mathbf{g} = \mathbf{l}|\mathbf{g}|$, but this point can be represented on the NT of the original PES, $V\,(\mathbf{r})$, where this NT is used for the pulling direction. The reason is that this special pulling direction does not change the description of this special NT on every effective PES under the pulling. An NT can start near both kinds of stationary points, minimums or saddle points in every direction. And it goes (usually, if no valley-ridge inflection point is met) from a minimum to an SP of index one, or vice versa (the last is the 'index theorem'[39]). In 'higher' regions of the PES regular NTs exist which connect SPs of index k and $(k+1)$, with $1 \leq k \leq N-1$, or vice versa.

If one moves on the path of FDSPs one has to increase the norm of the force, F, beginning at the original stationary points with $F = 0$ in the thermal limit: there is a part of the pathway from the minimum uphill, and a part from the SP downhill. Anywhere, if the force increases further and further, the two parts meet. Here the norm of the gradient has its maximum. Thus, the curvature of the PES along the corresponding NT is zero, because at the meeting point of the effective minimum and the SP we have $dV_f(\mathbf{r})/dt = \mathbf{l}^T\mathbf{A}\mathbf{l}(|\mathbf{g}| - F) = 0$.

As a consequence, the barrier of the original PES disappears. In other words, on the effective PES, $V_f(\mathbf{r})$, with the maximal rupture force,[40] the SP disappears, and the pulling force realizes the reaction. (This may happen somewhat earlier because of the existence of the zero point energy of the former minimum.) We propose to name the point the barrier breakdown point (BBP). Its necessary mathematical formula is[10,41]

$$Det(\mathbf{H}) = \mathbf{0} \ . \tag{6}$$

Note that $\mathbf{H}$ is always the Hessian of the original zero-force PES, $V(\mathbf{r})$, because the model Eqs.1 and 2 do not influence the calculation of the Hessian.[26] The idea of the proof of condition Eq.6 is that the BBP is a turning point of the function $|\mathbf{g}|$ along the NT. A proof of Eq.6 is given in ref. 10. The definition of an optimal pulling direction[10] is also derived: the mechanical force to be applied to the molecule of interest is $\mathbf{f} = F\,\mathbf{l}$ where $F = \sqrt{\mathbf{g}^T\mathbf{g}}$. To each NT belongs the corresponding $\mathbf{l}$-vector, and by varying it we have different NT curves. All the regular NTs, that leave the minimum and arrive at the same SP, cross at least once a $Det(\mathbf{H}) = 0$-line. The first $Det(\mathbf{H}) = 0$-line that each NT crosses gives the BBP of this NT, the maximal rupture force, F_{max}. This is due to the fact that at the BBP point of a regular NT, the gradient norm $|\mathbf{g}|$, takes its maximum value along this NT curve. If we compare all NTs of such a set, then the NT which gives the lowest value of F_{max} is named the *optimal NT*. It coincides with a gradient extremal (GE) exactly at the intersection point with the $Det(\mathbf{H}) = 0$-line.[10] In this special BBP, the $Det(\mathbf{H}) = 0$-line, the GE and the optimal regular NT meet. The optimal BBP is a stationary point on the function $|\mathbf{g}|$ crossed by the optimal NT. (In higher dimensional PESs, the condition $Det(\mathbf{H}) = 0$ may describe a manifold, but the GE and the NT are always one-dimensional curves.)

Historically, the BBP was named the breaking point distance (for single bonds),[14,40,42] and the corresponding magnitude F_{max} was named the rupture force. BBPs for bonds in diatomic molecules are calculated,[14,42,43] as well as the BBPs for single bonds in some polyatomics. The one-dimensional BBP-problem is also treated by Freund.[44] With the present model, both the BBP and F_{max} can be predicted for large molecules, thus in a higher dimension.

In the present study we will use optimal NTs on test surfaces to treat simple rate formulas under a pulling force. Recently, there is a paper by Zhuravlev et al.[19] where the authors

report an abnormal behavior of the $log(rate)$-curve, against the applied force, F. By simple 2-dimensional surface models with parallel reaction pathways representing competing reaction channels, we reproduce such an abnormal $log(rate)$-curve. By the simplicity of the test models, we can confirm some former explanations[45] for a counterintuitive behavior of some rate curves. It can emerge if the pulling changes the order of the SP-heights of the competing reaction channels. We emphasize that the present study uses generic PES models, associated with non-specific reaction mechanisms, to make the results as general as possible. Nevertheless, these generic surfaces are taken from well tested models of specific chemical systems.

The results are organized as follows. With 2-dimensional test surfaces we explain the impact of stress on the topography of the effective PES. First we treat the 'weakly multidimensional case'[19] with only one SP on the PES. In the next Subsection we give a possible explanation of abnormal $log(rate)$-curves over F in 'strong multidimensional cases'[19] with competing reaction pathways. The paper finishes with a Discussion and a Conclusion.

RESULTS

Potential energy surfaces with only one exit pathway

The skew-Morse minimum

We illustrate the concept of using NTs in more detail, with some test PESs, in the following 2-dimensional examples. The two coordinates used, (x, y), may be the plane of the two most important dimensions of a chemical reaction.[19] All other remaining coordinates are projected out of the treatment. It is further assumed that an important part of the pulling vector acts in this (x, y)-plane in any linear combination.[10,46] First we use an example of Ribas-Ariño and Marx[14] for a dissociating part of a molecule. The test PES is

$$V(x, y) = 100(1 - Exp[-x/\sqrt{2}\ ])^2 + 50y^2 - 25xy\ . \tag{7}$$

The Morse potential is assumed with dissociation energy, $D_e = 100$, and with force constant 25 in the neighborhood of the minimum. The y^2-term would be associated with

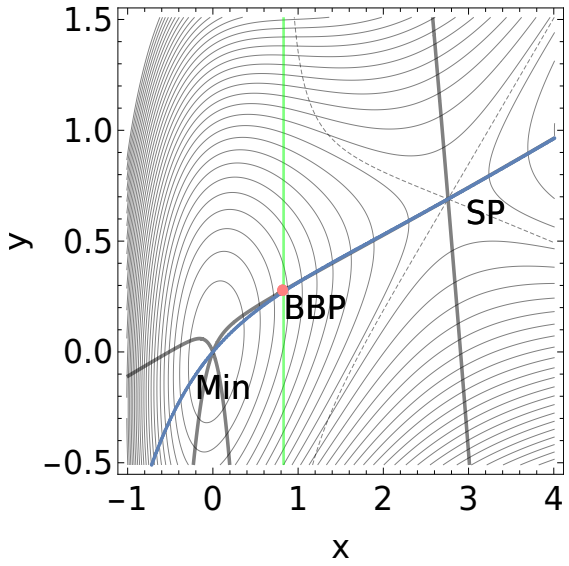

Figure 2: Surface of the PES of Eq.7 with the optimal NT (blue), the gradient extremal (thick black), and the BBP-line $Det(\mathbf{H}) = 0$ (green). The red point is the optimal BBP. Small dashes depict the convexity border of the PES.

an harmonic oscillator with a force constant of 100. The third term represents a coupling between the x and y coordinates causing a skew PES – skew means here that the SP does not lie in the direction of the normal modes of the minimum. The minimum is at zero level, but the SP is at height 49.8 energy arbitrary units. At the beginning we determine the optimal NT which has to cross the optimal BBP at (0.815,0.278). As explained in the previous section, it results by the crossing of a GE with the (green) force rupture line with condition $Det(\mathbf{H}) = 0$ which is here a straight line, see Fig.2. The gradient along the optimal NT points in the direction $\mathbf{l}_{opt}$=$(0.967,0.256)^T$.

Additionally to the optimal NT we use two further NTs for comparison, one is at the minimum steeper than the optimal NT, but nearby, with direction $\mathbf{l}_{upper}$=$(1,1)^T$ like in ref. 14. The other has an angle of more than 90^o to the optimal NT and has a turning point (TP) near the bottom of Fig.3. Its direction is $\mathbf{l}_{lower}$=$(0.477,-0.879)^T$.

However note that there is a limit direction, along a singular NT to a valley-ridge inflection point (not shown in Figs.2 and 3). Below such a direction a pulling does not exist which could overturn the minimum over the SP.[10] The BBP of the upper NT is at (0.815,0.445) but the BBP of the lower NT is at (0.815,-0.81). We assume that one can do a pulling

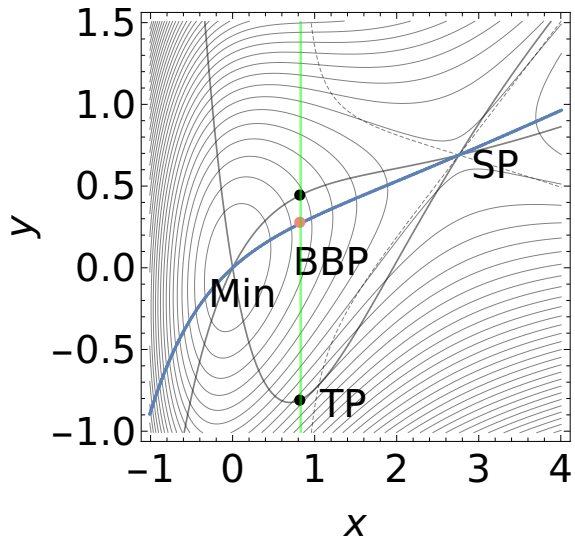

Figure 3: PES of Eq.7 with the optimal NT (blue), and two further NTs. The red point is the optimal BBP, two black points are the BBPs of the other NTs. The lower NT crosses the convexity border (thin dashes) at its turning point TP on the energy surface. Note that TP and BBP do not coincide in this example.

experiment into the three directions, $\mathbf{f}_{upper}$, $\mathbf{f}_{opt}$, and $\mathbf{f}_{lower}$, along the three directions of the NTs of interest. With different magnitude of the forces, F, along the three NTs, we get different effective PESs

$$V_F(x,y) = V(x,y) - F\ (l_x, l_y)\ (x,y)^T\ . \tag{8}$$

For fixed $\mathbf{l}$ and $\mathbf{f} = F\mathbf{l}$ we can slightly change the notation of $\mathrm{V}_f(x,y)$ to $\mathrm{V}_F(x,y)$ with respect to that employed in the introduction. We use for the upper NT: $0 \leq F \leq 33.8$, for the optimal NT: $0 \leq F \leq 28.8$, and for the lower NT: $0 \leq F \leq 115$; the upper limit is the corresponding rupture force of $|\mathbf{g}|$ at the BBPs.

We can determine the difference between the corresponding effective minimum and the effective SP for every F. Rates for forward reactions under the pulling forces are estimated by a simple Eyring-ansatz[14,24,47] for the activation energy on the effective PES

$$k_F = k_o Exp[-(V_F(SP) - V_F(Min))/kT] \tag{9}$$

where k_o is the Arrhenius preexponential factor of a reaction attempt frequency. We put

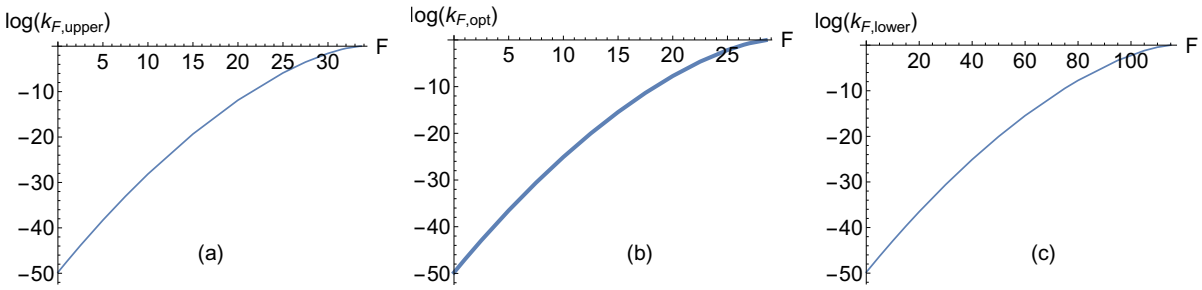

Figure 4: Semilogarithmic representation of Eyring rates 9 on the V_F surfaces of the skew Morse PES 7 over three pulling directions, see Fig.3. Note the different scaling of the force, F, which depends on the final BBP. Left panel (a): pulling along the upper NT, center (b): pulling along the optimal NT, right panel (c): pulling along the lower NT. All curves are regularly concave.

here the factor $k_o = 1$, and $kT = 1$, both in arbitrary units, for simplicity. We assume that the reaction occurs at a constant temperature.

Because of the different height of the three BBPs of this example, we need different scales for F. The result is shown in Fig.4. We get three 'normal' concave $log(k)$ curves increasing over F, independent on the pulling direction. 'Only' the F-scale is very different, in a ratio of 1:4, depending on the clever, or not so clever choice of the pulling direction. The effect of an increase of F on the effective stationary points, Min and SP, of the effective potential, V_F, results in a continuous decrease of $\Delta V_F = V_F(SP) - V_F(Min)$, for every allowed pulling direction. We remark that the $log(rate)$ curves are concave over F, thus they are regular as one expects it. The direction $(1,1)^T$ of ref. 14 is well guessed near the optimal direction.

The skew double-minimum PES [6,10]

We continue to use example 4 of ref. 10 We use a product of two quadratic forms

$$V(x,y) = (x-1, y-1) \begin{pmatrix} 1 & -1.11 \\ -1.11 & 3 \end{pmatrix} \begin{pmatrix} x-1 \\ y-1 \end{pmatrix} (x+1, y+1) \begin{pmatrix} 1 & 0 \\ 0 & 12.5 \end{pmatrix} \begin{pmatrix} x+1 \\ y+1 \end{pmatrix}. \tag{10}$$

The minimums lie at zero level, the SP is at level 24. We have the simplest case of two minimums, connected by one SP, compare ref. 23. The minimum at (-1,-1) be the reactant.

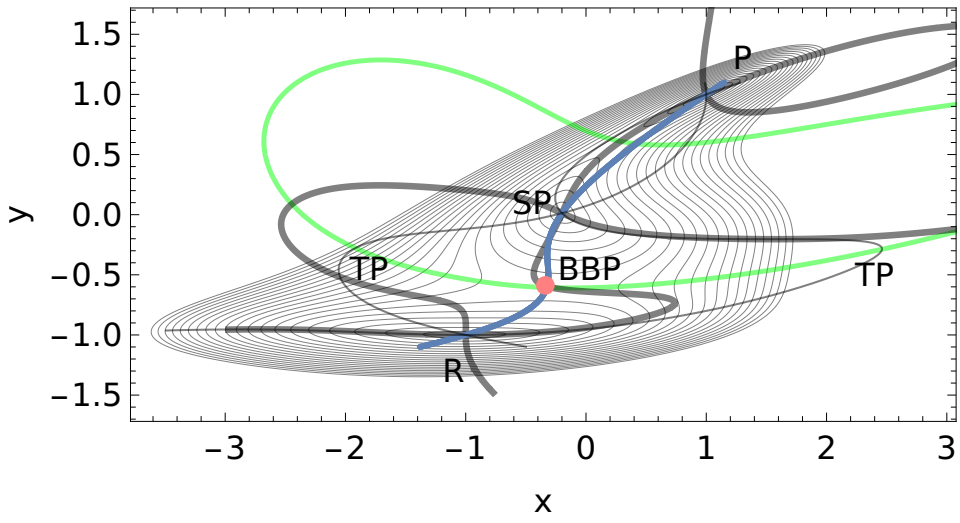

Figure 5: Surface of the norm of the gradient, $|\mathbf{g}|$, of the skew double-minimum PES of Eq.10. Included are the optimal NT (blue), two further NTs (thin black) with TPs, the gradient extremal (thick black), and the BBP-line $Det(\mathbf{H}) = 0$ (green), as well as the stationary points of the original PES of Eq.10. The red point is the optimal BBP. It is an SP of the $|\mathbf{g}|$-surface.

The minimum at (1,1) be the product. The optimal NT[10] crosses the minimal BBP at point (-0.338,-0.588). It is the crossing of the gradient extremal with the $Det(\mathbf{H}) = 0$ line. Here the surface of the norm of the gradient has an SP; see Fig.5. The BBP-line $Det(\mathbf{H}) = 0$ is a ridge on the surface $|\mathbf{g}| = \sqrt{\mathbf{g}^T\mathbf{g}}$ of the squared gradient, compare ref. 48. The lowest value of $|\mathbf{g}|$ on the ridge manifold in between the two valley-ridge inflection points is the optimal BBP. In the general case of an N-dimensional PES, the condition $Det(\mathbf{H}) = 0$ determines a manifold: the ridge manifold of $|\mathbf{g}|$.

We chose three NTs for an estimation of rates for three different pulling directions: one is the optimal NT (blue), and two NTs are side ways which are clearly not optimal, see Fig.6. (Compare also Figs. 5, 6, and 7 of ref. 10.) The constant gradient directions along the three NTs chosen are for the left NT $\mathbf{l}_{left}$=(-0.357,0.934)^T, for the optimal NT $\mathbf{l}_{opt}$=(0.259,0.966)^T, and for the right NT $\mathbf{l}_{right}$=(1,0)^T. As in the preceding example, with Eq.8 we use for the left NT: $0 \leq F \leq 94$, for the optimal NT: $0 \leq F \leq 32$, and we use for the right NT: $0 \leq F \leq 177$; where the limits are again the corresponding rupture forces, $F_{max} = |\mathbf{g}|_{max}$,

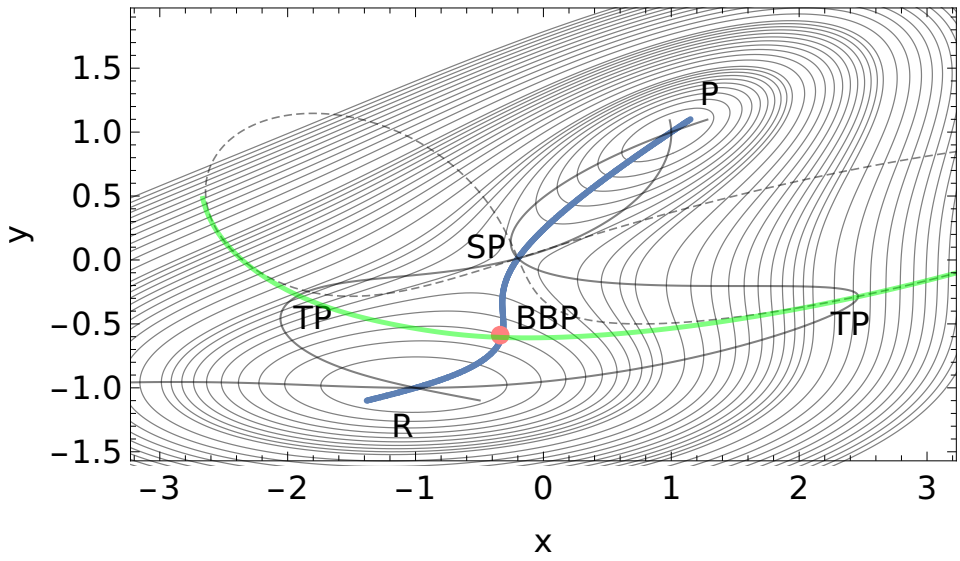

Figure 6: Surface of the skew double-minimum PES of Eq.10. We use different distances between the level lines: below, the distance is 4 levels (9 lines), then 10 steps follow with a step of 10, and the outer shell of level lines has steps of 25 levels (12 lines). The last shown level is at 450 units. Included are the optimal NT (blue) and two side NTs. The red point is the optimal BBP. The TPs of the side NTs are the BBPs of these NTs. They are at a height of 204 and 37.8 levels, correspondingly.

at the corresponding BBPs. Additionally, we assume no back reaction. Because of the very different heights of the three BBPs of the present case, we need different scales for F. The result for rates is shown in Fig.7. Representing $log(k)$ in front of F we obtain concave curves in the three cases. We note that this behavior is irrespective of the pulling direction. The F-scales are very different.

A **conclusion** for this Section is:
If model Eq. 1 is convenient for the pulling experiment, and if we have only one SP around the reactant valley, so to say, if it is a 'one-dimensional' problem on a higher-dimensional surface, then the overcoming of the SP is an intrinsic one-dimensional process along every of the possible NTs driven by the pulling. The pulling directions can point over a broad range.[10] The pulling can move the SP on the effective PES uphill into the original PES mountains, if the NT has a TP, however, because the minimum on the effective PES also moves uphill on

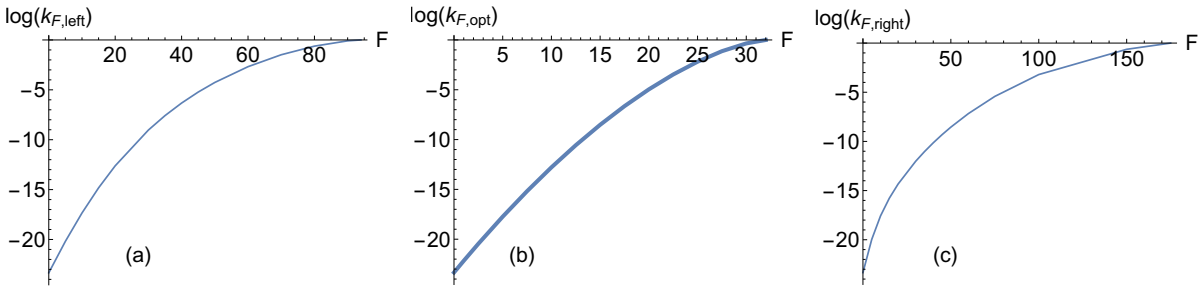

Figure 7: Semilogarithmic representation of Eyring rates of Eq.9 on the V_F surfaces of the skew double-minimum PES of Eq.10 over three pulling directions, see Fig.6. Note the different scaling of the force, F, depending on the final BBP. Left panel (a): pulling along the left NT, center (b): pulling along the optimal NT, right panel (c): pulling along the right NT. All curves are regularly concave.

the original PES, nevertheless, the differences of both energies usually become smaller. The behavior is named transition state stabilization in enzyme catalysis.[49] So to say, for a fixed F, the effective SP and the effective minimum do not move equidistantly. Compare Fig.8, for at least this representative example. Though the PES may be higher-dimensional, the pulling process is only 'weakly multidimensional'.[19] The form of the $log(k)$ curve over F does not show indications of a catch-bond behavior, compare ref. 45. Remember: for a catch-bond behavior the dissociation lifetime increases with the applied force. Here, the probabilistic chemistry on the current effective PES, V_F, 'normally' goes its intuitive way where a bond is slipped by the pulling. We underline that both of the examples result with qualitatively equal $log(k)$-curves, compare Figs.4 and 7. Fig.4 may concern a dissociation, but Fig.7 may concern an isomerization. This is not a mathematical proof for such curves. In comparison, the present results differ somewhat with respect to that reported in ref. 50 for NTs with TPs, compare Fig.1.B there. It is also not consistent to the 'rollover'-result for a one-exit PES in refs. 31 and 51. We found that a TP of the pulling NT has only an influence on the rupture force, F_{max}. In the case of the right NT, F_{max} is 5 times larger than the rupture force of the optimal direction. But we find no qualitative change of the pulling process. Generally, it is known that the reduction to a one-exit model is a huge simplification,[30] which may be only of theoretical interest.

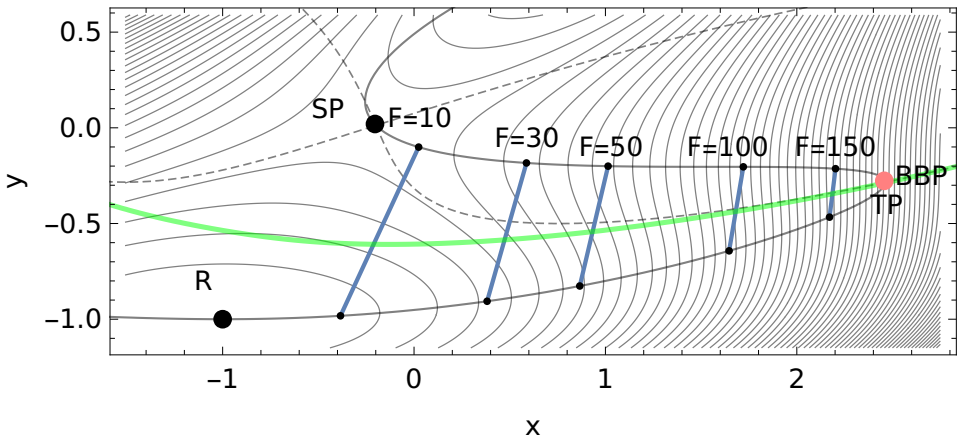

Figure 8: Pulling along the right NT on the double-minimum PES of Eq.10. Here we use equidistant level lines of the PES. Included is the right NT from R over a TP and along a ridge back to the SP. (This NT is clearly not the optimal NT between R and SP.) The red point is its force rupture BBP. Here it is the TP of the NT. The included sticks represent the connections between the effective SPs (above on the ridge) and the effective minimums (below in the valley) at the indicated pulling forces, F, correspondingly. The effective stationary points are indicated by black points. For comparison, the background PES is the PES in the thermal limit, $F = 0$. See the text for a detailed explanation.

Potential energy surfaces with parallel pathways

The Rhee-Pande PES[52]

The next example is a model for a two-pathway surface[45,53] where we assume that the directed mechanical force, $\mathbf{f}$, enables a reaction pathway which is energetically disfavored in the forceless case.[35] Of course, the two-pathway-model is still in the framework of minimal models[31] as well. The example may be understood as topological extract of a chemical example for pulling scenarios[19] where the high molecular dimension of the problem is projected into two intrinsic dimensions. It concerns a protein folding in a β-sandwich protein, the G-gallus src SH3 domain from Tyr kinase. Of course, this is a simplified model. Further examples for a two-pathway surface, thus the existence of catch-bonds, can be found,[20,33,50,53–67] to name just a few. We treat a 2-dimensional test surface of Rhee and Pande[52] for the case of competing RPs. Additionally, on the lower path emerges an intermediate minimum, compare

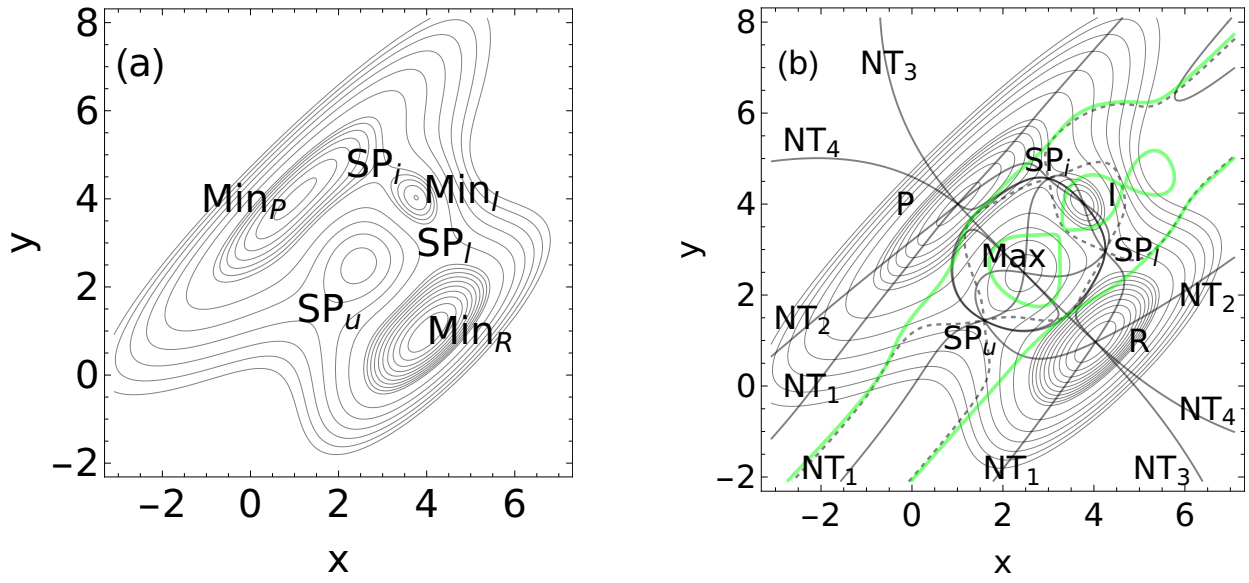

Figure 9: (a)The Rhee-Pande surface.[52] Levels start at zero. The lower, first energy levels are in 1-steps; but after level 10, the higher levels go in 5-steps. (b) Four NTs: two optimal NTs for a pulling: NT_1 and NT_2, and two singular NTs: NT_3 and NT_4. The dashed curves give the valley-ridge borders. The green curves are the BBP condition det(**H**)=0.

ref. 68. The expression of this PES is

$$V(x,y) = (1 - 0.5\ Tanh[y-x])\ (x+y-5)^2 + 0.2 * (((y-x)^2-9)^2 + 3\ (y-x)) \qquad (11)$$

$$+15\ Exp[-(x-2.5)^2-(y-2.5)^2] - 20\ Exp[-(x-4)^2-(y-4)^2] + 1.67318\ .$$

There are three minimums (reactant, intermediate, and product), three SPs (the low SP_l, the upper SP_u, and the SP behind the intermediate, SP_i), and a maximum at the center, see Fig.9. The relations between the stationary points become clear by the following numbers: reactant at 0 energy units, intermediate at 5.963 energy units, product at 3.637 energy units, low SP_l at 12.842 energy units, upper SP_u at 24.003 energy units, and intermediate SP_i at 9.573 energy units. Thus, the upper reaction pathway is approximately twice in energy than the height of the lower reaction path.

With the result of the former Section, we know that we can restrict our treatment on the optimal NTs. The two 'optimal' NTs for a pulling, here named NT_1 and NT_2, are

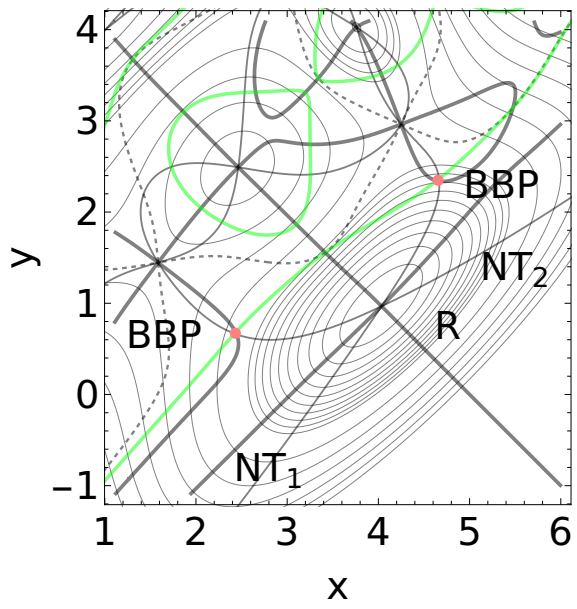

Figure 10: GEs on the Rhee-Pande surface (fat lines). The intersection (red points) with the green line in the reactant valley gives the two optimal BBPs. The green curves depict the condition det(**H**)=0. The two optimal NTs for a pulling: NT_1 and NT_2 are the NTs which also intersect these BBPs.

derived by the intersection of gradient extremals (GEs) with a green line, see the red points in Fig.10. Their two directions are $\mathbf{l}_1$=(-0.076,0.997)^T and $\mathbf{l}_2$=(-0.943,0.333)^T. They show an interesting difference, an asymmetry on this surface: One branch of the NT_1 goes after the start at the reactant to the SP_l, crosses the intermediate, and turns after the SP_i uphill through the maximum. Then it leaves the region after crossing of the SP_u on a ridge. It does not reach the product: there is another branch of this NT_1 through the product.

In contrast, NT_2 connects all stationary points: if starting at the reactant, it goes to SP_u, then to the maximum, after this it steps down to the SP_l, turns to the intermediate, and goes at least through the SP_i to the product. Note that both of the optimal NTs lead over the SP of index two, here a maximum. Thus, when we study the pulling problem by NTs, we have to include these higher index SPs, compare ref. 71.

On the other hand, the singular NTs, NT_3 and NT_4, also represent the slight asymmetry of the surface. NT_3 bifurcates at the VRI point between the two SP-valleys of the product side, while NT_4 bifurcates at the VRI point between the two SP-valleys of the reactant

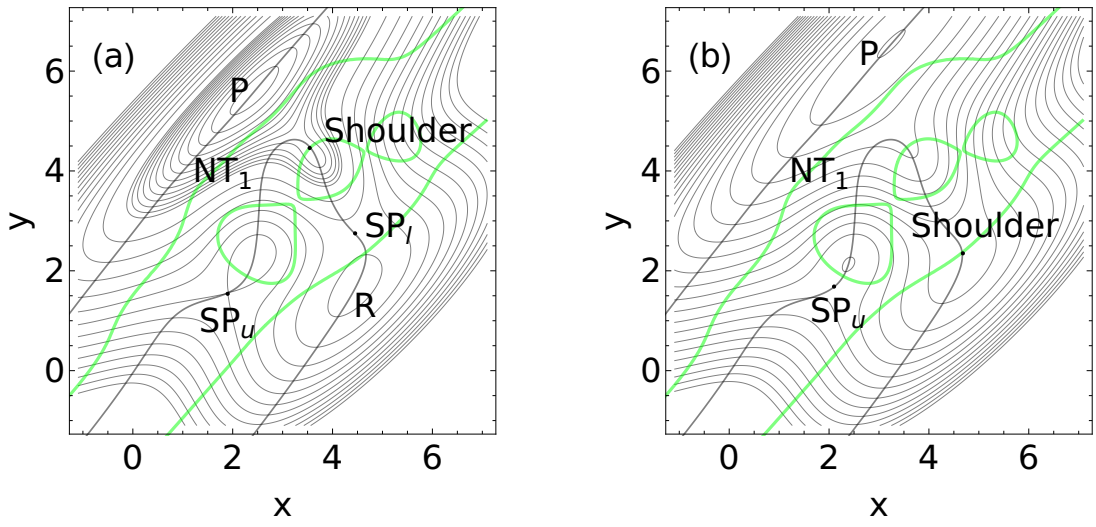

Figure 11: Two cases of V_F of the Rhee-Pande PES for two pulling forces, (a) $F = 6.625$ and (b) $F = 10.511$ along NT_1: first, (a) the SP_i coalesces with the intermediate to a shoulder.[69,70] Levels start at -27 units here. The lower, first energy levels are in 1-steps up to -15 units; but after this level, the higher levels go in 5-steps up to 50 units. Later, in panel (b), the SP_l coalesces with the reactant minimum to a shoulder. There is the final BBP of the PES. Here the levels start at -50 units at P and they go in in 5-steps up to 50 units. Note that the effective PES changes with F, however, the used NT_1 and the lines $Det(\mathbf{H}) = 0$ (green) survive all linear pullings of model Eq. 1. In this case, a flat SP_u still remains on the PES.

side. Their two directions are $\mathbf{l}_3$=(-0.714,0.7)^T and $\mathbf{l}_4$=(-0.694,0.72)^T. (We do not show the valley-ridge inflection points in Figs. 9 and 10.)

If we assume a pulling along the corresponding direction of the two optimal NTs, $\mathbf{l}_1$=(-0.076,0.997)^T or $\mathbf{l}_2$=(-0.943,0.333)^T, we get the movement of the corresponding stationary points on the new effective potentials. The pulling along NT_1 is shown in Fig.11; such a schematic sequence of effective PESs, V_F, is proposed in refs. 21,31.

We get a similar picture for a pulling along the NT_2 as is shown in Fig.12.

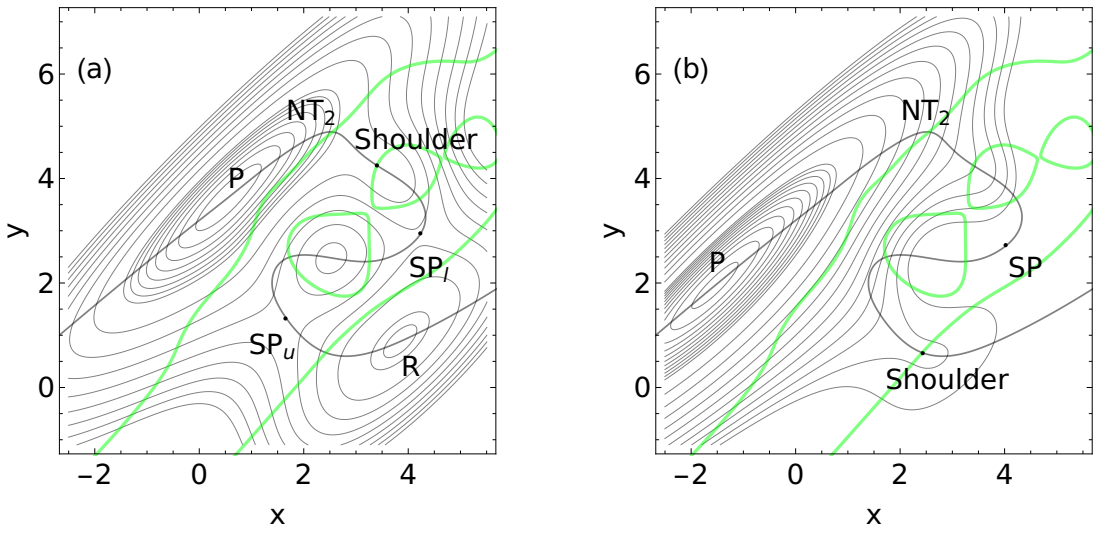

Figure 12: Two cases of V_F of the Rhee-Pande PES for two pulling forces, (a) $F = 2.5$ and (b) $F = 15.092$ along NT_2: first, (a) again the SP_i coalesces with the intermediate to a shoulder. The levels are like in the case $F = 0$. Later, (b) the SP_u coalesces with the reactant minimum to a shoulder. There is now the final BBP of the PES. The former minimum disappears, but the former SP_l still remains on the PES. Levels start at -15 units here. The lower, first energy levels are in 1-steps up to -5 units; but after this level, the higher levels go in 5-steps up to 50 units.

Conclusion

If model Eq. 1 is convenient for the pulling experiment, then every of the two competing valleys for a reaction $R \rightarrow P$ of the Rhee-Pande PES, Eq. (11), can be enforced by a corresponding special pulling direction. It is demonstrated here along the optimal NTs to the two SPs. The intermediate of the Rhee-Pande PES does not play a special role.

The conclusion is consistent with the calculated molecular examples of Lenhardt et al.[72] to the ring opening of *gem*-difluorocyclopropanes, of Ong et al.[20] for the ring opening of cyclobutene, and of Bailey and Mosey[34] to the ring opening of 1,3-cyclohexadiene. They attained that a given force, $\mathbf{f}$, can guide the system along specific cis- or disrotatory reaction pathways. Other examples are reported elsewhere.[73,74]

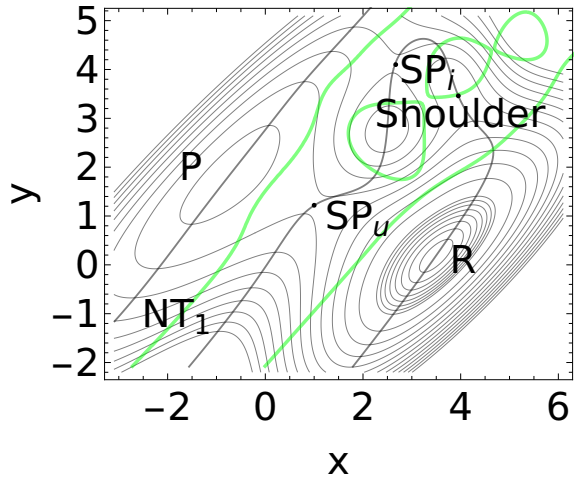

Figure 13: V_F of the Rhee-Pande PES for pulling force, $F = 8.5$ backwards along NT_1: the SP_l coalesces with the intermediate minimum to a shoulder. Levels are like in the $F = 0$ case. The SP_i and SP_u remain, but they change their order. None of the valleys totally disappears, either.

An interesting detail of the NT_1 of the Rhee-Pande PES

In the case of this chosen PES, we still find an interesting detail. If one studies the back reaction, then the contrary pulling along NT_1 could be associated to a compression of a molecule.[72,75,76] The process here has to have forces in direction $-l_1 = (0.076, -0.997)$, however, it cannot reach a final BBP, because the branch of the NT_1 through the product minimum does not cross the green line of the product valley, see Figs.9(b) and 11. So to say, this direction is a forbidden direction for the back reaction. For $F = 8.5$ the intermediate coalesces with the SP_l, however, the SP_i remains in the valley, see Fig.13. The former SP_u is already the lower barrier. At this point, a larger reaction rate for a back reaction will use the channel over the former SP_u. But this picture also remains for still stronger forces: only the product wanders to the left hand side along the product branch of NT_1, cf. Fig.13. Thus, we can totally overpower the reactant by a strong force into the product, along NT_1; however, we cannot totally overturn the product back by any strong inverse force along NT_1. Of course, under other pulling directions, corresponding NTs exist which allow a full overturn of the product valley, P, for example, to the inverse NT_2.

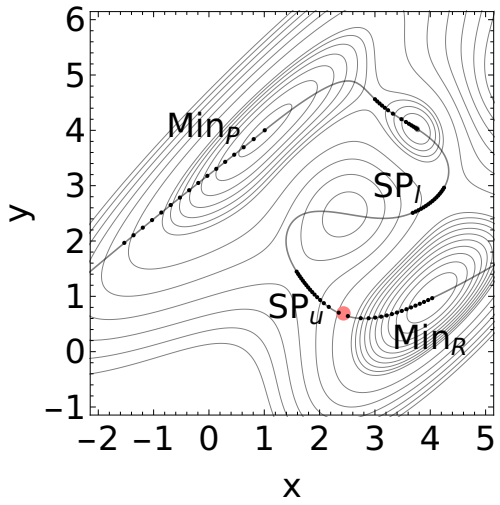

Figure 14: Stationary points of diverse V_F surfaces of the Rhee-Pande PES, Eq.11, for pulling forces, $F = 0, 1, ..., 15$ along the direction of NT$_{up}$. Compare Fig.12. The red point is the BBP of this direction. The level lines of the original PES for F=0 are shown as the background. They indicate the initial stationary points.

Rates for reactions along the two RPs

We calculate the forward rates of a reaction for the optimal NT$_{up}$=NT$_2$ to the SP_{up}. We use the simple Eyring-ansatz[47] on the effective PES like Eq.9

$$k_{F,up} = k_{o,up} Exp[-(V_F(SP_{up}) - V_F(Min))/kT] \ , \tag{12}$$

and analogously, it may hold for the rates of a reaction for the SP_{low}

$$k_{F,low} = k_{o,low} Exp[-(V_F(SP_{low}) - V_F(Min))/kT)] \tag{13}$$

where $k_{o,up}$ and $k_{o,low}$ are factors of a reaction attempt frequency. We put here the factors $k_{o,..} = 1$ arbitrary units, and $kT = 1$ arbitrary units, for simplicity. Eqs.12 and 13 mean that we use the true energy difference of the corresponding effective SP and the effective minimum. Thus, we go back from an approximative Bell-ansatz[77] to Eyring[24,47] on V_F. Our use of a simple model-based PES allows an explicitly defined forward rate. Additionally it is known that the Bell-model fails in the description of rate constants under high forces.[78] Note, we assume no back reaction; it is adapted to the reference 19 of comparison of this

work, where the first passage times of trajectories at the product are counted. No back trajectories are used.

Note that all stationary points move with increasing force, F, along the NT chosen, say the $\mathrm{NT}_{up} = NT_2$. To illustrate this movement, we show in Fig.14 all stationary points of the diverse effective PESs, V_F, for $\mathbf{l}_{up}$ and F=0,1,...,15, embedded in the original PES, compare also Fig.12. It is clear that all stationary points on the diverse effective PESs move along the NT of the pulling experiment.

For a common reaction rate over both SPs we have the linear sum of both rates, thus it results in

$$k_F = \; k_{F,up} + k_{F,low} \; . \tag{14}$$

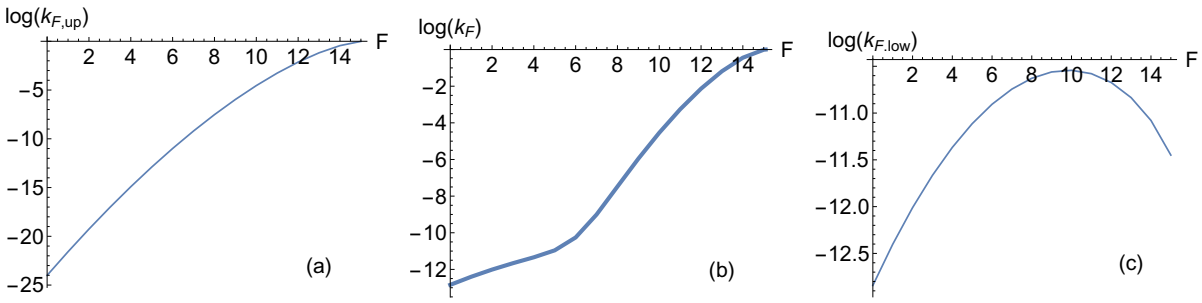

Figure 15: Semilogarithmic representation of Eyring rates on diverse V_F surfaces of the Rhee-Pande PES, Eq.11,[52] over the pulling force, F, in the direction of NT_{up}. Left panel (a): exit over original SP_{up}, center (b): k_F with Eq.14, right panel (c): exit over original SP_{low}.

Fig.15 shows the result for the pulling direction of NT_{up}=NT_2. Fig.16 shows the result for the pulling direction of NT_{low}=NT_1. In the latter case, the lower SP_l is the exit for the pulling process; it will be the lower SP throughout, down to its disappearance. The very small rate over the upper SP_{up} (Fig.16(a)) does not play any role. So to say, the overcoming of the SP is here a one-dimensional process along the NT_{low} driven by the pulling. Though the PES is two-dimensional, the process is only 'weakly multidimensional'.[19] The second dimension over the second SP_u does not play a role.

However, in the former case, the pulling process will go over the original upper SP_u. The relation of the two SPs can change along the pulling. Here the following happens: anywhere,

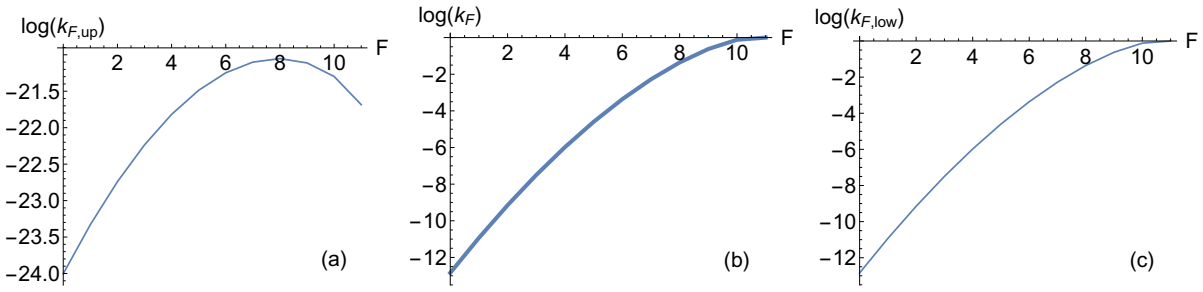

Figure 16: Semilogarithmic Eyring rates on diverse V_F surfaces of the Rhee-Pande PES, Eq.11, over the pulling force, F, in the direction of NT_{low}. Left panel (a): exit over original SP_{up}, center (b): k_F with Eq.14, right panel (c): exit over original SP_{low}.

the former upper SP becomes the lower one. At the end it coalesces with the reactant minimum. The very low rate at the initial forces, F=0,1,...,5 crosses at $F \approx 6$ the rate of the former lower SP_l (Fig.15(c)). The crossing results in a kink in the $log(rate)$ over all two SPs, see Fig.15(b). The kink emerges because there are at least two dimensions for the pulling force: this aspect of a claim of ref. 19 is correct. However, the upward curvature is not caused by the dimension of the problem alone. We see this in Fig.16(b) on the same PES. The kink has its reason in the pulling direction which points to a higher SP exit of the reactant valley. That causes a crossing of the SP heights. "The slip barrier must be higher than the catch barrier".[45] The curvature of the $log(rate)$-curve against the force, $\mathbf{f}$ depends on the relation of $\mathbf{f}$ to the currently lowest SP of the PES valley. Of course, this problem can only emerge for more than a one-dimensional reaction coordinate.

The experimental result with a proteine in Fig.2 C of ref. 19 shows a quite similar shape of the kink of the $log(rate)$-curve like our Fig.15(b). Note another spacing in our case which finishes at $log(k) = 0$ at the force rupture end.

The modified Eckhardt-PES[79]

We treat a second two-pathway example. We are interested in a simple template for the experimental/computational rates of Fig.2 of ref. 25 or Fig.4 of ref. 80. The first is the enforced ring opening of cyclopropane, the second concerns a pulling experiment for the

cleavage of a disulfide bond in an immunoglobulin-like domain of titin. There the rate decreases first with increasing force, up to a certain kink, where it again increases. We treat a test surface modified after Eckhardt[79] for the case of two competing RPs, Fig.17. The expression is

$$V(x,y) = 10(\frac{1}{2}Exp[-x^2-(y+1)^2] + \frac{3}{2}Exp[-x^2-(y-1)^2] + 4Exp[-\frac{3}{2}(x^2+y^2)] \quad (15)$$

$$+0.3y^2 + 0.002x^3 + (x/3)^4 - 0.177016) \ .$$

There is again an asymmetry for the two minimums associated to the reactant and the product, the two SPs, the low SP_{low} and the upper SP_{up}, and a maximum at the center, see Fig.17. The relations between the stationary points become clear by the following numbers: the reactant is at zero energy, the product is at 0.228 energy arbitrary units, the low SP_l at 10.244 energy arbitrary units, the upper SP_u at 15.845 energy arbitrary units, and the maximum, the SP_{index2} is at 45.86 energy arbitrary units. The upper reaction pathway is the higher reaction path. Here the intermediate is missing. In comparison to the former example, the central maximum is much higher.

We chose the optimal NT_1 to the upper SP, see Fig.17, for a pulling. It is derived by the intersection of a gradient extremal (GE) with a green line of the reactant valley, see the red points in the figure. The gradient direction along the NT_1 is (0.663, 0.774). It crosses the BBP_1 of this direction at point (-1.175, 1.668). Pulling along the NT_1 leads to the BBP_1 at F=8.257. Here, the upper SP and the reactant coalesce. On the other side of the PES, the lower SP and the maximum move together, thus, the barrier height of the lower SP increases under this pulling direction. It causes a strong decrease of the rate over this former lower SP, compare Fig.18(c).

Other optimal NTs lead to the other minimal BBPs. The BBP_2 at point (0.984,-1.33) is met by the direction $(-0.761,-0.649)^T$ of an NT_2. The two NTs, NT_1 and NT_2, are very similar. They dismiss their diagonal BBP by a small distance only, compare Fig.17 for NT_1. The same holds for a pair of two other optimal NTs which lead to the minimal BBP_3 and BBP_4. The points are at (-0.987, -1.325) and (1.163, 1.675); and the directions of the optimal NTs are $(0.772, -0.635)^T$ and $(-0.63, 0.777)^T$.

To qualitatively estimate the rates, we use Eqs.12, 13, and 14. We get the expected

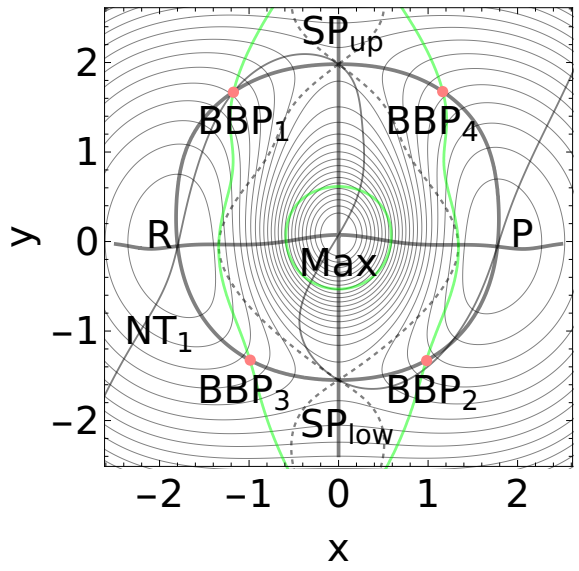

Figure 17: GEs on the modified Eckhardt surface (fat lines). The intersections (red points) with the green lines give the optimal BBPs. The green curves depict the condition $det(\mathbf{H}) = 0$. The optimal NT for a pulling over SP_{up}, NT_1, is the NT which also intersects the left upper BBP_1.

behavior for the $log(rate)$ over the force with Fig.18: however, here we find not only a kink, but a decreasing curve at the beginning. The decrease holds as long as the former lower SP does not become the higher barrier. Then the main stream of a reaction goes over the former upper SP and we approximate a 'normal' behavior of the reaction rate with a slipping bond. The emergence of the rate-turnover, compare Fig.4 of ref. 80 and our Fig.18 (b), is a hint of the existence of the peptide PES with (at least) two competing parallel reaction pathways. The force of the pulling modulates the behavior of the protein environment surrounding the cleaved disulfide bond[80] in (at least) one further dimension.

DISCUSSION

NTs describe the FDSPs of a pulling. The NTs on a PES are discriminated by the emergence of VRIs, valley-ridge inflection points.[10] All directions of regular NTs in between the singular NTs to two neighbor VRIs are allowed for a pulling scenario. This also holds in the N-dimensional case of the PES: the VRIs together with the singular NTs compose mani-

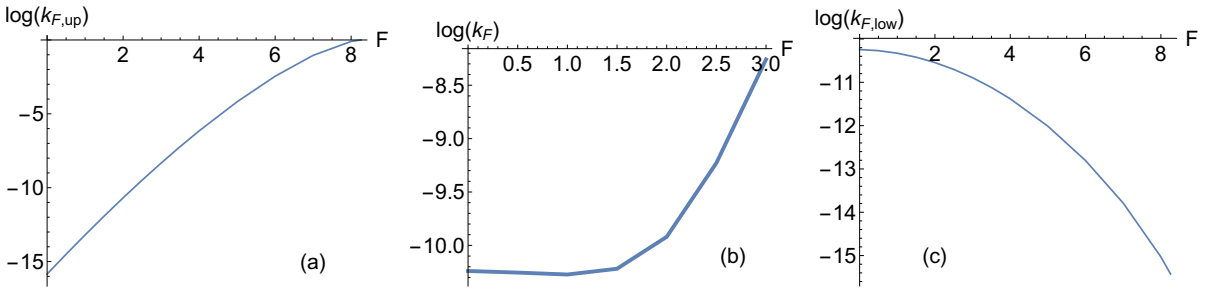

Figure 18: Eyring rates on diverse V_F surfaces of the modified Eckhardt PES, Eq.15, over the pulling force, F, in the direction of NT_1. Left panel (a): exit over original SP_{up}, center (b): k_F with Eq.14, right panel (c): exit over original SP_{low}.

folds which partition the full configuration space for NTs.[2,36] The VRI points determine the pulling channels.[39] NTs form a family of dense curves over the configuration space. Around every stationary point, into all directions of a possible force, $\mathbf{l}$, an NT starts. The range of all adapted directions for an NT family to a given SP is a range of useful forces of a mechanochemical pulling scenario for the molecule. Changing from one NT-family to another behind a VRI point corresponds to a reaction mechanism switch.[41,81]

The mechanical force tilts the PES. The calculation of the corresponding SPs on many consecutive surfaces V_F can be reduced to the curve following along the NT on the original, zero-force PES, V, in direction $\mathbf{l}$, up to the corresponding force $|\mathbf{g}|_{max} = F_{max}$ of the final BBP. To follow an NT in an N-dimensional space is a possible task, using Eq.3, because it is a one-dimensional curve which we can follow.[2,6,7] The NT-tool works well in any number of dimensions. All stationary points of an FDSP curve of the different effective PESs are obtained automatically, if one follows the corresponding NT. There is no need for a new calculation of any SP on the different effective potentials which was already remarked by Avdoshenko and Makarov.[82]

If there is more than one SP around a minimum for parallel paths to the product, and if the pulling direction points to an SP having not the lowest exit barrier, then diverse barriers of the PES can change their order under the pulling force. The ensemble of SPs undergoes

dramatic shifts.[19] In such a case we can get an abnormal, piecewise convex $log(rate)$-curve, seen over the amount of the force, F, of the pulling. For large molecules with many degrees of freedom it is improbable that a technical pulling direction points to the 'lowest' SP around the reactant minimum valley.[50] Of course, the used Eqs.12, 13, and 14 are very simple models for a forward rate. Maybe they oversimplify the reality; but a Smoluchowski equation for a more realistic behavior of the molecule,[80] for example, has also to use any kind of rates like Eqs.12 and 13 as an input. Then, the result may be a somewhat smoothed rate; but the qualitative shape of the curve will be conserved. The $log(rate)$ curves show that the mechanical force and the thermal activation act in concert with each other.[76]

Note that this work is a theoretical treatment using only the geometry of a projected PES near an interesting reactant minimum. Elementary chemical reactions rarely exceed $1\,nm$ of the movement of the included atoms while mechanochemical models often involve the directional translation at a lengthscale of up to $1\,\mu m$.[13] Of course, there are much more dimensions included into the pulling process than the two dimensions of interest treated here. We only pitch on the part of the pulling in the 2-dimensional plane of interest. One should compare ref. 83 for a discussion apart from the two-state restriction of our simple model. Additionally, the mechanism through which the force, $\mathbf{f}$, is transmitted to the molecule[12,46,72] is not considered here. We assume that the molecule can sustain a sufficient large force.[84] For simplicity, we have assumed that the direction of the force, $\mathbf{f}$, is constant. For nonlinear angle- and distance-coordinates, this may be an oversimplification. However, a local change of the direction, $\mathbf{l}$, whould only change the locally used NT, but the theory of its application in Eq.1 would endure. The used rate model ansatz is very simple, however, it qualitatively reproduces some found, 'counterintuitive' experimental results.

CONCLUSIONS

Newton trajectories on the original PES can be used for a model of the 'reaction path following force displaced stationary points' of every developed effective PES under a pulling force, or under the action of a catalytic environment of a molecule with an electrostatic

force, **f**. We continously assume that the model Eq.1 is in accordance with the pulling experiment. Especially, the kind of curves of Newton trajectories forms an important model for the treatment of mechanochemistry or catalysis including the reaction rates. Newton trajectories (NT) and Thom's[69,70] Catastrophe theory for the barrier breakdown point can be used for the analysis. The theory of NTs is well prepared. We have demonstrated that competing NTs over different SPs can cause an 'abnormal' upward $log(rate)$-curve under a corresponding pulling direction.

ACKNOWLEDGMENT

We are grateful to Prof. J. Ribas-Ariño for encouragement and helpful discussions.
There was no financial support for this paper.

References

1. W. Quapp, M. Hirsch, O. Imig, and D. Heidrich, J. Comput. Chem. **19**, 1087 (1998).
2. W. Quapp, M. Hirsch, and D. Heidrich, Theor. Chem. Acc. **100**, 285 (1998).
3. J. M. Anglada, E. Besalú, J. M. Bofill, and R. Crehuet, J. Comput. Chem. **22**, 387 (2001).
4. J. M. Bofill and J. M. Anglada, Theor. Chem. Acc. **105**, 463 (2001).
5. R. Crehuet, J. M. Bofill, and J. M. Anglada, Theor. Chem. Acc. **107**, 130 (2002).
6. W. Quapp, J. Theoret. Comput. Chem. **2**, 385 (2003).
7. W. Quapp, J. Molec. Struct. **695–696**, 95 (2004).
8. J. Bofill and W. Quapp, J. Chem. Phys. **134**, 074101 (2011).
9. W. Quapp and J. Bofill, J. Phys. Chem. B **120**, 2644 (2016).
10. W. Quapp and J. M. Bofill, Theoret. Chem. Acc. **135**, 113 (2016).

11. M. K. Beyer and H. Clausen-Schaumann, Chem. Rev. **105**, 2921 (2005).

12. M. M. Caruso, D. A. Davis, Q. Shen, S. A. Odom, N. R. Sottos, S. R. White, and J. S. Moore, Chem. Rev. **109**, 5755 (2009).

13. T. J. Kucharski and R. Boulatov, J. Mater. Chem. **21**, 8237 (2011).

14. J. Ribas-Ariño and D. Marx, Chem. Rev. **112**, 5412 (2012).

15. P. Baláž, M. Achimovičová, M. Baláž, P. Billik, Z. Cherkezova-Zheleva, and et al., Chem. Soc. Rev. **42**, 7571 (2013).

16. J. Wang, T. B. Kouznetsova, Z. Niuand, M. T. Ong, H. M. Klukovich, A. L. Rheingold, T. J. Martinez, and S. L. Craig, Nat. Chem. **7**, 323 (2015).

17. D. E. Makarov, *Single Molecule Science: Physical Principles and Models* (CRC Press, Taylor & Francis Group, Boca Raton, 2015).

18. D. E. Makarov, J. Chem. Phys. **144**, 030901 (2016).

19. P. I. Zhuravlev, M. Hinczewski, S. Chakrabarti, S. Marqusee, and D. Thirumalai, Proc. Natl. Acad. Sci. **113**, E715 (2016).

20. M. T. Ong, J. Leiding, H. Tao, A. M. Virshup, and T. J. Martínez, J. Am. Chem. Soc. **131**, 6377 (2009).

21. J. Ribas-Ariño, M. Shiga, and D. Marx, Angew. Chem., Int. Ed. **48**, 4190 (2009).

22. K. Wolinski and J. Baker, Molec. Phys. **107**, 2403 (2009).

23. S. M. Avdoshenko and D. E. Makarov, J. Phys. Chem. B **120**, 1537 (2015).

24. H. Eying, J. Walter, and G. E. Rimball, *Quantum Chemistry* (John Wiley and Sons, Inc., New York, 1944).

25. P. Dopieralski, P. Anjukandi, M. Rückert, M. Shiga, J. Ribas-Ariño, and D. Marx, J. Mater. Chem. **21**, 8309 (2011).

26. E. R. Thornton, J. Am. Chem. Soc. **89**, 2915 (1967).

27. R. Groote, R. T. M. Jakobs, and R. P. Sijbesma, Polymer Chem. **4**, 4846 (2013).

28. Y. Tian and R. Boulatov, Chem. Commun. **49**, 4187 (2013).

29. O. K. Dudko, G. Hummer, and A. Szabo, Physical review letters **96**, 108101 (2006).

30. R. B. Best, E. Paci, G. Hummer, and O. K. Dudko, J. Phys. Chem. B **112**, 5968 (2008).

31. Y. Suzuki and O. K. Dudko, J. Chem. Phys. **134**, 065102 (2011).

32. S. S. M. Konda, J. M. Brantley, C. W. Bielawski, and D. E. Makarov, J. Chem. Phys. **135**, 164103 (2011).

33. M. Krupička and D. Marx, J. Chem. Theory Comput. **11**, 841 (2015).

34. A. Bailey and N. J. Mosey, J. Chem. Phys **136**, 044102 (2012).

35. M. Gensler, C. Eidamshaus, A. Galstyan, E.-W. Knapp, H.-U. Reissig, and J. P. Rabe, J. Phys. Chem. C **119**, 4333 (2015).

36. W. Quapp, J. Math. Chem. **54**, 137 (2015).

37. F. H. Branin, IBM J. Res. Develop. **16**, 504 (1972).

38. I. H. Williams and G. M. Maggiora, J. Mol. Struct. (Theochem) **89**, 365 (1982).

39. M. Hirsch and W. Quapp, J. Molec. Struct., THEOCHEM **683**, 1 (2004).

40. M. K. Beyer, J. Chem. Phys. **112**, 7307 (2000).

41. S. S. M. Konda, S. M. Avdoshenko, and D. E. Makarov, J. Chem. Phys **140**, 104114 (2014).

42. J. Ribas-Ariño, M. Shiga, and D. Marx, J. Am. Chem. Soc. **132**, 10609 (2010).

43. M. F. Iozzi, T. Helgaker, and E. Uggerud, Mol. Phys. **107**, 2537 (2009).

44. L. B. Freund, Proc. Nat. Acad. Sci. **106**, 8818 (2009).

45. O. V. Prezhod and Y. V. Perevzev, Acc. Chem. Res. **42**, 693 (2009).

46. A. L. Black, J. M. Lenhardt, and S. L. Craig, J. Mater. Chem. **21**, 1655 (2011).

47. H. Eyring, J. Chem. Phys. **3**, 107 (1934).

48. J. Duncan, Q. Wu, K. Promislov, and G. Henkelman, J. Chem. Phys. **140**, 194102 (2014).

49. A. Warshel, P. K. Sharma, M. Kato, Y. Xiang, H. Liu, and M. H. M. Olsson, Chem. Rev. **106**, 3210 (2006).

50. S. S. M. Konda, J. M. Brantley, B. T. Varghese, K. M. Wiggins, C. W. Bielawski, and D. E. Makarov, J. Am. Chem. Soc. **135**, 12722 (2013).

51. Y. Suzuki and O. K. Dudko, Phys. Rev. Lett. **104**, 048101 (2010).

52. Y. M. Rhee and V. S. Pande, J. Phys. Chem. B **109**, 6780 (2005).

53. V. Barsegov and D. Thirumalai, Proc. Natl. Acad. Sci. **102**, 1835 (2005).

54. K. K. Sarangapani, T. Yago, A. G. Klopocki, M. B. Lawrence, C. B. Fieger, S. D. Rosen, R. P. McEver, and C. Zhu, J. Biol. Chem. **279**, 2291 (2004).

55. C. Zhu, J. Lou, and R. P. McEver, Biorheology **42**, 443 (2005).

56. C. Zhu and R. P. McEver, Molec. Cell. Biomech. **2**, 91 (2005).

57. V. Heinrich, A. Leung, and E. Evans, J. Chem. Inf. Model. **45**, 1482 (2005).

58. O. V. Prezhod, O. V. Prezhdo, W. E. Thomas, and E. V. Sokurenko, Phys. Rev. E **72**, 010903 (2005).

59. O. V. Prezhod, O. V. Prezhdo, M. Forero, E. V. Sokurenko, and W. E. Thomas, Biophys. J. **89**, 1446 (2005).

60. Y. V. Perevzev, E. Prezhdo, and E. V. Sokurenko, Biophys. J. **101**, 2026 (2011).

61. W. E. Thomas, Curr. Nanosci. **3**, 63 (2007).

62. W. E. Thomas, V. Vogel, and E. Sokurenko, Annu. Rev. Biophys. **37**, 399 (2008).

63. J. B. Udgaonkar, Annu. Rev. Biophys. **37**, 489 (2008).

64. B. Jagannathan, P. J. Elms, C. Bustaments, and S. Marqusee, Pros. Nat. Acad. Sci. **109**, 17820 (2012).

65. S. M. Kreuzer, T. J. Moon, and R. Elber, J. Chem. Phys. **139**, 121902 (2013).

66. P. Dopieralski, J. Ribas-Arino, P. Anjukandi, M. Krupička, and D. Marx, Angew. Chem. Int. Ed. **55**, 1304 (2016).

67. M. F. Pill, S. W. Schmidt, M. K. Beyer, H. Clausen-Schaumann, and A. Kersch, J. Chem. Phys. **140**, 044321 (2014).

68. A. Garai, Y. Zhang, and O. K. Dudko, J. Chem. Phys. **140**, 135101 (2014).

69. R. Thom, *Structural Stability and Morphogenesis: An Outline of a General Theory of Models* (Addison-Wesley, Reading, MA, 1989).

70. D. Heidrich, W. Kliesch, and W. Quapp, *Properties of Chemically Interesting Potential Energy Surfaces* (Springer, Berlin, Heidelberg, 1991).

71. W. Quapp and J. M. Bofill, Int. J. Quantum Chem. **115**, 1635 (2015).

72. J. M. Lenhardt, A. L. Black, B. A. Beiermann, B. D. Steinberg, F. Rahman, T. Samborski, J. Elsakr, J. S. Moore, N. R. Sottos, and S. L. Craig, J. Mater. Chem. **21**, 8454 (2011).

73. E. Evans, A. Leung, H. Volkmar, and C. Zhu, Proc. Natl. Acad. Sci. **101**, 11281 (2004).

74. V. Blanco, D. A. Leigh, and V. Marcos, Chem. Soc. Rev. **44**, 5341 (2015).

75. S. R. Jezowski, L. Zhu, Y. Wang, A. P. Rice, G. W. Scott, C. J. Bardeen, and E. L. Chronister, J. Am. Chem. Soc. **134**, 7459 (2012).

76. S. W. Schmidt, P. Filippov, A. Kersch, M. K. Beyer, and H. Clausen-Schaumann, ACS Nano **6**, 1314 (2012).

77. G. I. Bell, Science **200**, 618 (1978).

78. W. Li and F. Gräter, J. Am. Chem. Soc. **132**, 16790 (2010).

79. B. Eckhardt, Physica D **33**, 89 (1988).

80. M. Roy, G. Grazioli, and I. Andricioaei, J. Chem. Phys. **143**, 045105 (2015).

81. Z. T. Yew, M. Schlierf, M. Rief, and E. Paci, Phys. Rev. E **81**, 031923 (2010).

82. S. M. Avdoshenko and D. E. Makarov, J. Chem. Phys **142**, 174106 (2015).

83. H. Lannon, E. Vanden-Eijnden, and J. Brujic, Biophys. J. **103**, 2215 (2012).

84. G. S. Kochhar and N. J. Mosey, Scientific Reports **6**, 23059 (2016).